Journal of Food Engineering 190 (2016) 195–204

Contents lists available at ScienceDirect

Journal of Food Engineering

journal homepage: www.elsevier.com/locate/jfoodeng

Effect of mixing on LAOS properties of hard wheat flour dough

Gamze Yazar [a, b], Ozlem Caglar Duvarci [a, c], Sebnem Tavman [b], Jozef L. Kokini [a, *]

[a] Purdue University Food Science Department, 745 Agriculture Mall, Dr West Lafayette, IN 47907, USA
[b] Ege University Food Engineering Department, Ege University Campus, Bornova, Izmir, Turkey
[c] Izmir Institute of Technology, Department of Chemical Engineering, Urla, Izmir, Turkey

ARTICLE INFO

Article history:
Received 16 December 2015
Received in revised form
30 April 2016
Accepted 19 June 2016
Available online 21 June 2016

Keywords:
LAOS parameters
Non-linear rheology
Lissajous-Bowditch curves
Hard wheat flour dough
Farinograph mixing

ABSTRACT

Large Amplitude Oscillatory Shear (LAOS) tests were conducted at strains ranging from 0.01% to 200% and different frequencies (20, 10, 1, and 0.1 rad/sec) on hard wheat flour dough samples obtained from the different phases of Farinograph mixing: 1) at the first peak, 2) 5 min after the first peak, 3) 12 min after the first peak, 4) at the 20th min. All samples showed strain stiffening and shear thinning behavior in large strains. The gluten network is the origin of strain stiffening behavior and the rearrangement of the suspended starch matrix is the origin of shear thinning behavior. LAOS enables us to independently deconvolute these two events offering new insights into the structural origins of rheological properties in the non-linear region. Dough samples started to show strain softening and shear thickening after giving a peak around 100% strain due to the onset of the breakdown of the gluten network.

1. Introduction

Dough's rheological response to large deformations is of particular importance (Amemiya and Menjivar, 1992; Schulentz et al., 2000; Connelly and Kokini, 2007; Kim et al., 2007). Strains experienced by dough during mixing and in the bread-making process can range from 100% during sheeting to 1000% during fermentation and oven rise, and up to 500,000% during mixing (Menjivar, 1990). Fundamental rheological measurements in the nonlinear region using Large Amplitude Oscillatory Shear (LAOS) tests may be useful. Ewoldt and McKinley through the elegant use of Fourier transforms coupled with Chebyshev polynomials developed sound rheological properties to be able to characterize viscoelastic rheology in the non-linear region (Ewoldt et al., 2007; Hyun et al., 2011; Ewoldt, 2013; Liu et al., 2014). This method is based on Fourier transform rheology (FT-rheology) (Wilhelm, 2002; Klein et al., 2008; Nam et al., 2010; Wilhelm, 2011). For a sinusoidal strain input $\gamma(t) = \gamma_0 \sin(\omega t)$, the stress response can be represented completely by a Fourier series given in two alternate forms to emphasize either elastic or viscous scaling, respectively.

$$\sigma(t;\omega,\gamma_o) = \gamma_o \sum_{nodd} \{G'_n(\omega,\gamma_o)\sin n\omega t + G''_n(\omega,\gamma_o)\cos n\omega t\} \text{ (for elastic scaling)},$$

$$\sigma(t;\omega,\dot{\gamma}_0) = \dot{\gamma}_0 \sum_{nodd} \{\eta''_n(\omega,\gamma_0)\sin n\omega t + \eta'_n(\omega,\gamma_0)cosn\omega t\} \text{ (for viscous scaling)}.$$

Here, ω is the imposed oscillation frequency, γ_0 is the strain amplitude, $\dot{\gamma}_0$ the resulting strain rate, and t is time (Ewoldt et al., 2008).

The stress response in LAOS is not sinusoidal in the non-linear region; the stress response wave is not proportional to the applied strain wave and the linear viscoelastic functions, G′ and G″, do not have any useful meaning. In the nonlinear region, the storage and loss modulus become a function of the strain amplitude as well as the applied frequency (G′ ($\gamma_{0,\omega}$) and G″ ($\gamma_{0,\omega}$)) (Nam et al., 2010; Hyun et al., 2011).

Ewoldt et al. (2008) extended the method of orthogonal stress decomposition used previously by Cho et al. (2005) in order to soundly interpret LAOS data. This method decomposes the generic nonlinear stress response into a superposition of an elastic stress $\sigma'(x)$, where $x = \gamma/\gamma_0 = \sin\omega t$ and viscous stress $\sigma''(y)$, where $y = \dot{\gamma}/\dot{\gamma}_0 = \cos\omega t$. The sum of these elastic and viscous contributions is expressed as the total oscillatory stress, $\sigma(t) = \sigma'(t) + \sigma''(t)$. They are

* Corresponding author.
E-mail address: jkokini@purdue.edu (J.L. Kokini).

http://dx.doi.org/10.1016/j.jfoodeng.2016.06.011
0260-8774/

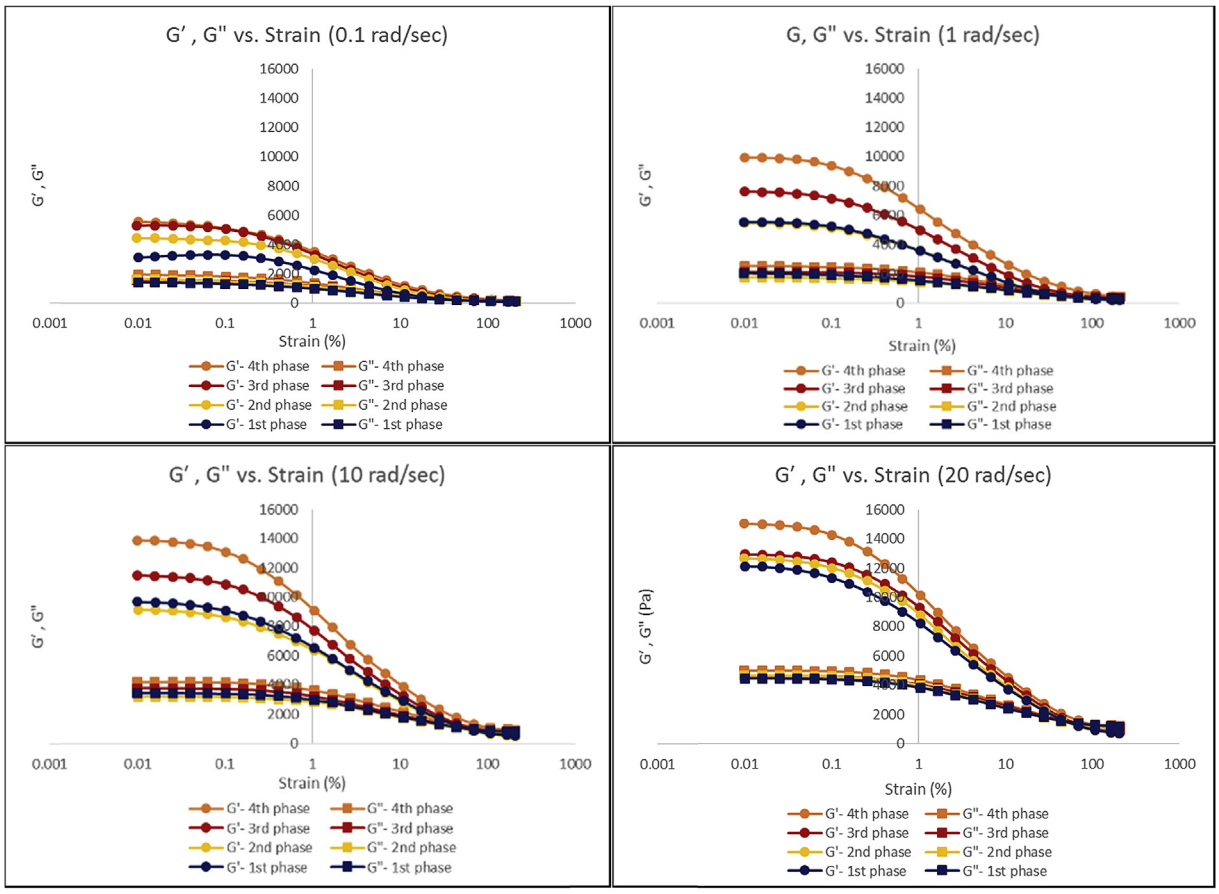

Fig. 1. G values of hard dough samples.

related to the Fourier decomposition as indicated below:

$$\sigma' \equiv \frac{\sigma(\gamma,\dot{\gamma}) - \sigma(-\gamma,\dot{\gamma})}{2} = \gamma_0 \sum_{nodd} G'_n(\omega,\gamma_0)\sin n\omega t,$$

$$\sigma'' \equiv \frac{\sigma(\gamma,\dot{\gamma}) - \sigma(\gamma,-\dot{\gamma})}{2} = \gamma_0 \sum_{nodd} G''_n(\omega,\gamma_0)\cos n\omega t.$$

The elastic and viscous contributions to the measured stress response are then obtained as follows;

$$\sigma'(x) = \gamma_0 \sum_{n:odd} e_n(\omega,\gamma_0)T_n(x), \sigma''(y)\sigma''(x)$$
$$= \dot{\gamma}_0 \sum_{n:odd} v_n(\omega,\gamma_0)T_n(y),$$

$T_n(x)$ represents the nth-order Chebyshev polynomial with odd symmetry and $x = \gamma/\gamma_0, y = \dot{\gamma}/\dot{\gamma}_0$ provide the appropriate domains of $[-1, +1]$ for orthogonality. Ewoldt et al. (2008) very astutely recognized that $e_n(\omega,\gamma_0)$ represented the elastic Chebyshev coefficients and $v_n(\omega,\gamma_0)$ the viscous Chebyshev coefficients.

$$e_n = G'_n(-1)^{(n-1)/2} \quad n : odd,$$

$$v_n = \frac{G''_n}{\omega} = \eta'_n \quad n : odd.$$

The raw periodic stress response $\sigma(t;\omega,\gamma_0)$ at steady state is plotted parametrically against $\gamma(t)$ after the stress data is normalized for the amplitude of stress (σ/σ_o) and the strain data is normalized for the amplitude of strain (γ/γ_o). These plots are commonly called Lissajous-Bowditch curves and they display characteristic transitions in the non-linearity of the fluid's response. In the linear region, the shape of the Lissajous graph is elliptic in the elastic analysis. In the nonlinear region, a deformed parallelogram is observed whose shape depends on the applied strain and the frequency during the deformation process.

The application of LAOS to characterize the large amplitude nonlinear rheological properties of food products is new. Examples include gluten gels (Ng et al., 2011), polysaccharide dispersions i.e.

Table 1
Crossover points for hard wheat flour dough samples at different phases of Farinograph mixing.

Frequency (rad/sec)	1st phase of mixing	2nd phase of mixing	3rd phase of mixing	4th phase of mixing
	Strain (%)			
0.1	52.79 ± 3.20	87.80 ± 10.99	175.13 ± 14.07	177.24 ± 63.72
1	49.99 ± 3.90	65.80 ± 6.63	101.45 ± 7.27	201.46 ± 12.27
10	57.35 ± 2.96	55.66 ± 0.71	78.12 ± 5.59	113.58 ± 12.54
20	50.12 ± 8.85	57.56 ± 5.76	51.52 ± 17.70	94.17 ± 21.18

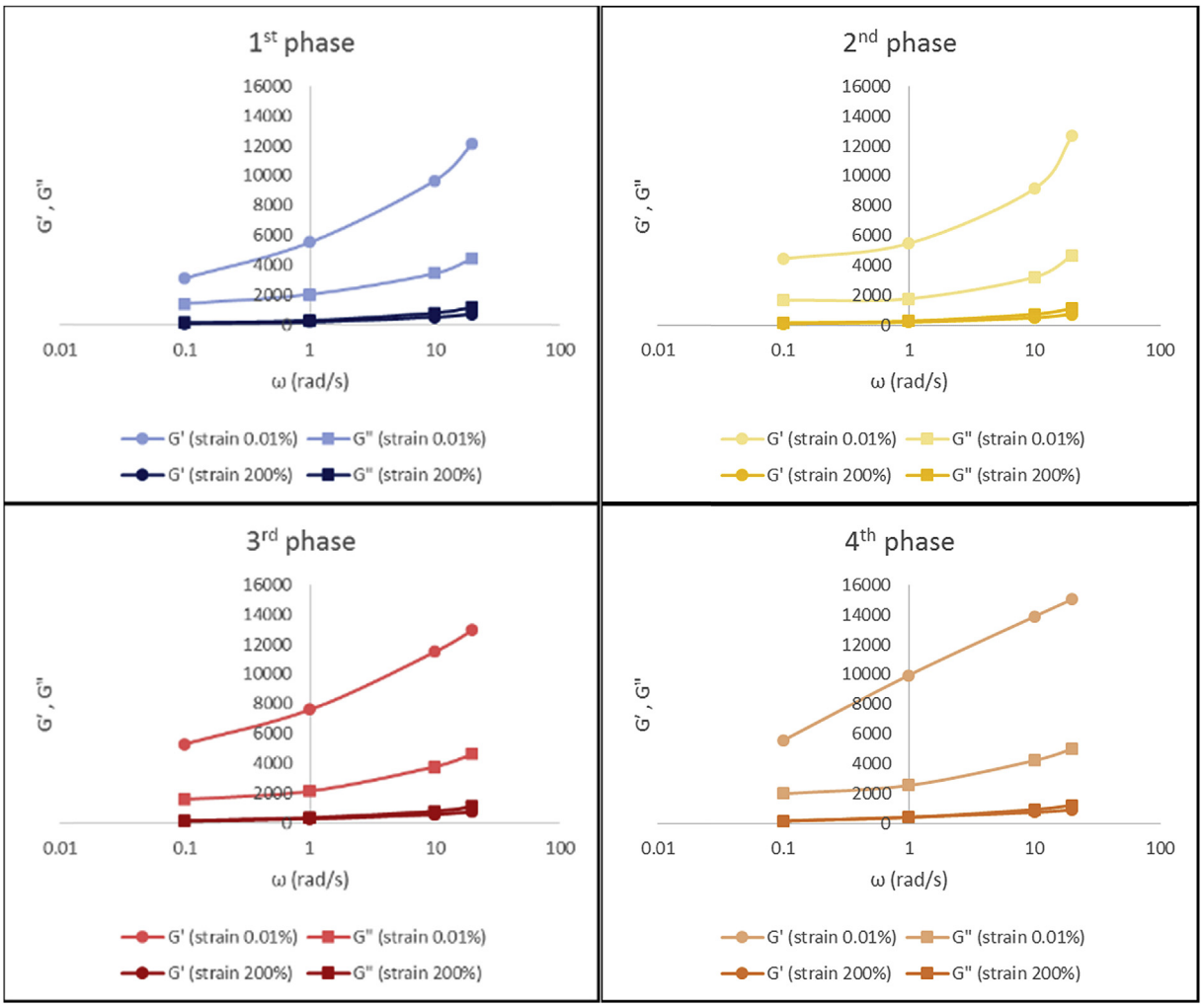

Fig. 2. G values of hard dough samples at the highest (~200%) and the lowest (~0.01%) strain values.

carrageenan or starch (Klein et al., 2008), whey protein isolate and κ-carrageenan gels (Melito et al., 2013a), tuna myofibrillar protein (Liu et al., 2014), commercial cheese (Melito et al., 2013b), and tomato paste (Duvarci et al., 2016). Because the technique offers new intracycle information at each strain studied, it gives deeper insights previously unavailable through the use of linear viscoelastic rheological analysis.

The objective of this research is to study the nonlinear rheological properties of hard wheat flour dough as a function of mixing time in a Brabender Farinograph, report the changes that occur in the stress waveform as strain is increased, plot intracycle behavior using Lissajous curves, obtain the Chebyshev constants and help understand the molecular origins from inferences that can be drawn from earlier studies.

2. Materials and methods

2.1. Materials

Hard red winter wheat flour (11.54% moisture, 29.8% wet gluten, 63.3% water absorption) obtained from Siemer Milling Company (Hopkinsville, KY) was used to prepare the dough samples evaluated in this study.

2.2. Methods

Dough samples were prepared using a Farinograph (Brabender, Germany) according to the AACC method 54-21 (AACC, 2000). The Farinograph torque values were recorded as a function of time during mixing.

The non-linear rheological properties of the dough samples were measured with a DHR-3 Rheometer (TA Instruments, USA) using the LAOS (Large Amplitude Oscillatory Shear Test) mode. The measurements were carried out in triplicate at 25 °C using frequencies of 0.1, 1, 10, 20 rad/sec and between the strain values of 0.01 and 200% at nine values of strain. A 40 mm sand-blasted plate and a gap of 2 mm were used for all the measurements. The dough samples were rested until the axial normal force relaxed to 1 N. All the non-linear data were obtained through the use of TRIOS software provided by TA for LAOS analysis. The raw stress waves and Lissajous curves were drawn using the software OriginPro 8.6.

3. Results and discussion

3.1. Raw rheological data for hard wheat flour dough

3.1.1. Dough development data during mixing

The Farinograph curves show a strong and resilient dough with excellent stability. The arrival time is equal to 0.5 min the peak time

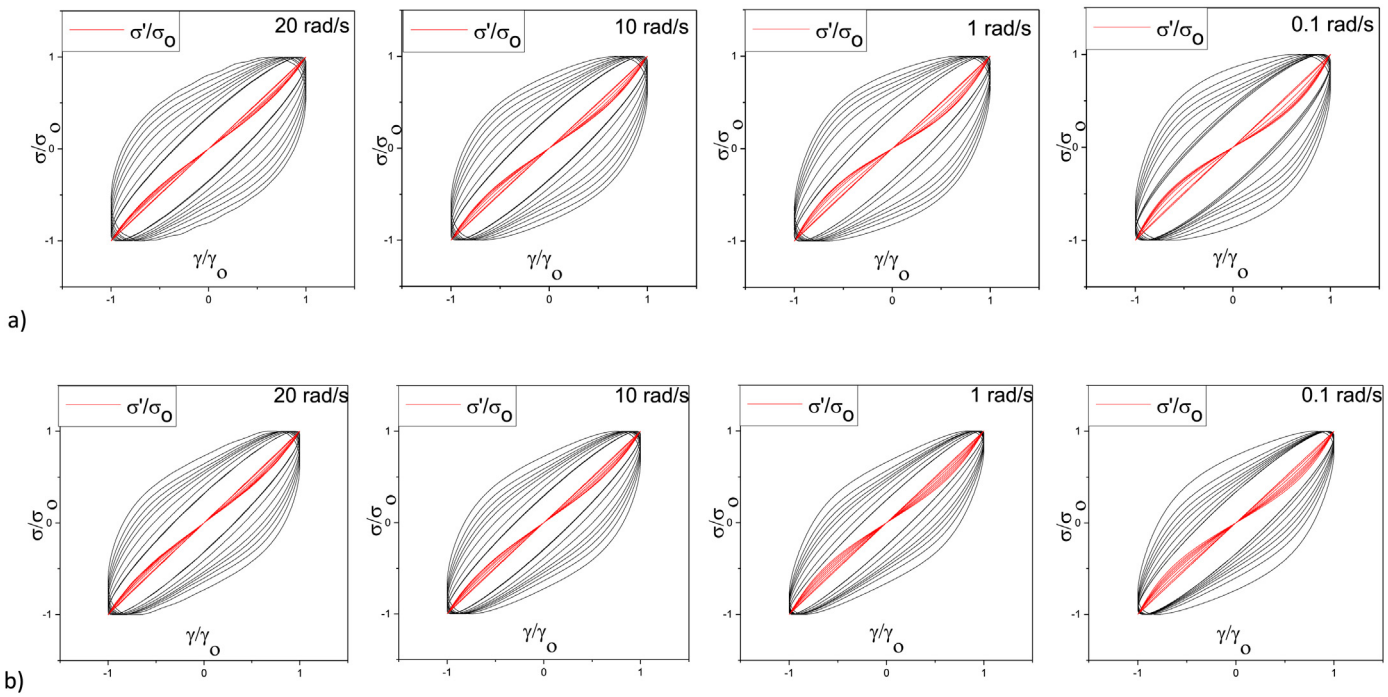

Fig. 3. Lissajous curves for the elastic component of hard wheat flour dough obtained from a) the 1st phase of Farinograph mixing and b) the 4th phase of Farinograph mixing.

is 9.0 min. The departure time is > 20 min and the stability of the dough is equal to 16.0 min. In order to study the effect of mixing on LAOS properties, wheat flour dough samples were obtained at 4 different stages of Farinograph mixing: 1) at the first peak, right after the arrival time at 1.25 min (1st phase), 2) 5 min after the first peak, before the peak time, 3) 12 min after the first peak, after the peak time, 4) at 20 min, which corresponds to where we stopped Farinograph mixing measurement (standard procedure).

3.1.2. Analysis of the rheological behavior in the linear and non-linear region

Analysis of the rheology of the hard wheat flour dough samples was carried out at strains corresponding to the SAOS, medium LAOS (MAOS) and LAOS regions (0.01, 0.06, 1.6, 11, 28, 44, 70, 105, and 200%). G′ and G″ values were evaluated in SAOS, whereas LAOS rheological parameters were evaluated in the non-linear region.

Fig. 1 shows the linear G′ and G″ values at different stages of

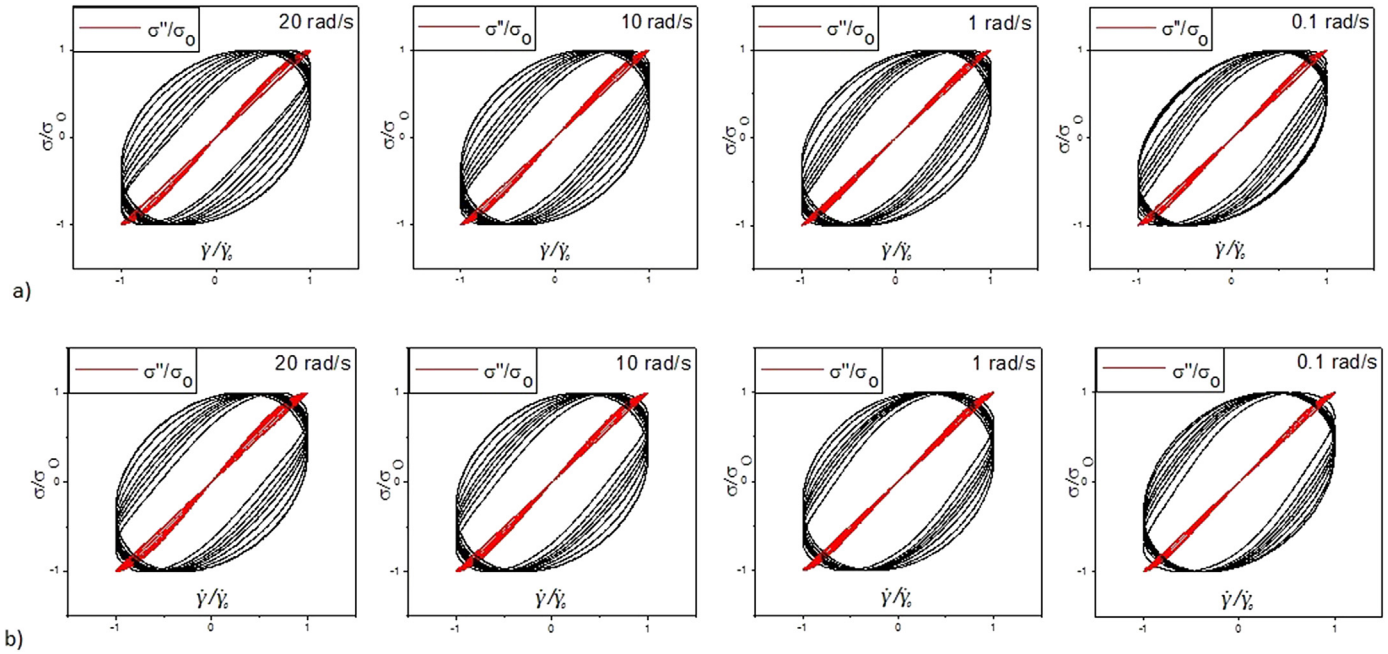

Fig. 4. Lissajous curves for the viscous component of hard wheat flour dough obtained from a) the 1st phase of Farinograph mixing and b) the 4th phase of Farinograph mixing.

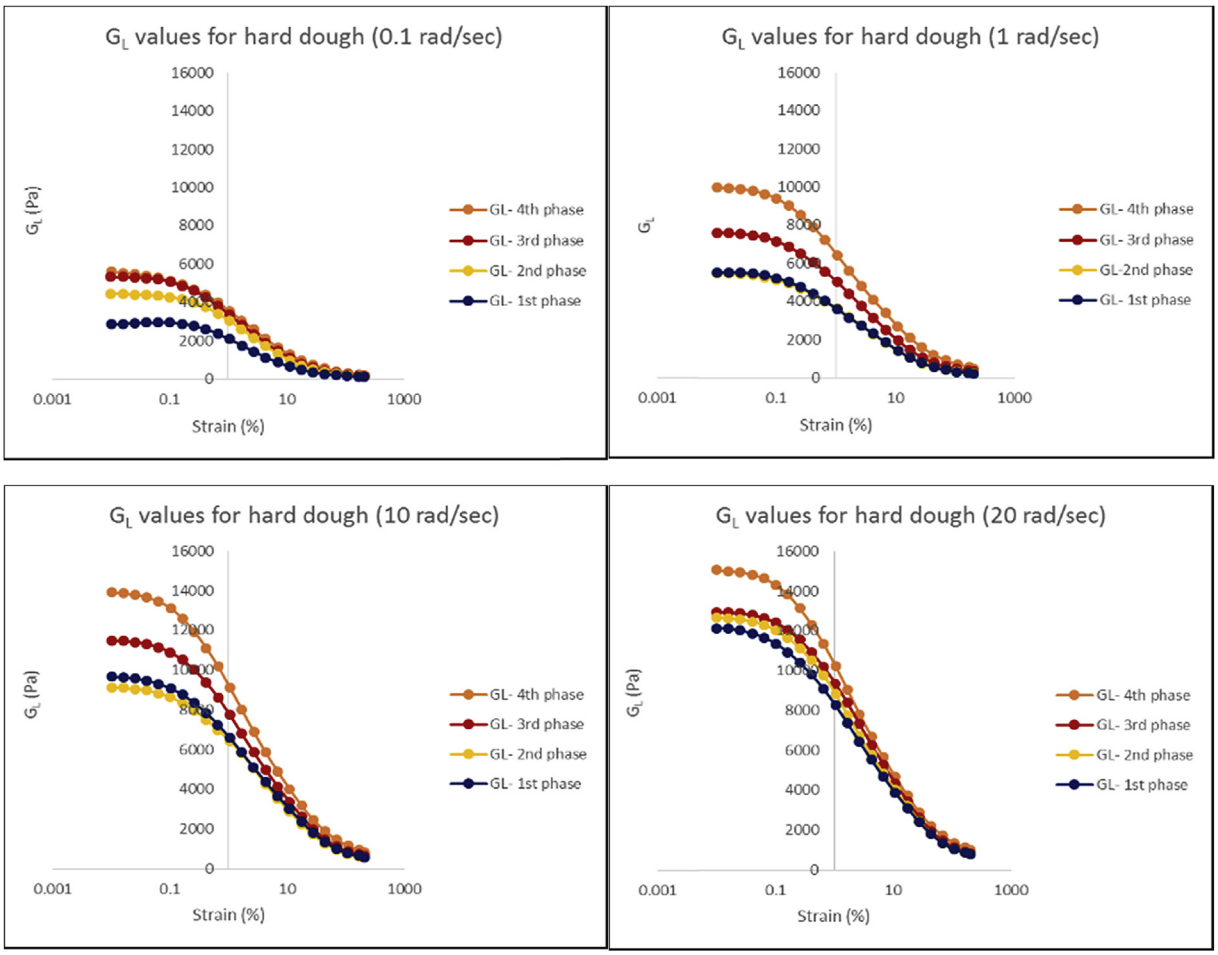

Fig. 5. Large strain modulus (G_L) values for hard dough samples.

Farinograph mixing. At a strain of 0.01% and a frequency level of 0.1 rad/sec, the dough sample from the 1st phase of mixing had the lowest G′ value whereas the dough samples from the 3rd and the 4th phases of mixing had similar and highest G′ values. At the highest frequency of 20 rad/sec the dough sample from the 4th phase of the mixing again showed the highest G′ value while the dough samples from the 1st, 2nd, and 3rd mixing phases showed lower and relatively close G′ values. All these observations suggest that the protein network continued to develop throughout the four phases of mixing. The more developed network structure induced by mixing showed more elasticity indicated by higher G′ value. When the frequency is higher, the energy delivery to the sample happens in a shorter period of time which results in the cross over of G′ and G″ in smaller strains. Clearly, this is the outcome of the high 16 min long stability of hard wheat flour dough.

We observe that the transition strain is relatively large at small frequencies (0.1 and 1 rad/sec) and becomes progressively lower as the frequency increases (10 rad/sec and 20 rad/sec) showing that the gluten network is unable to maintain its network structure and disulfide bonds holding it together begin to breakdown under the magnitude of the increasing stress injecting a level of energy exceeding the maximum stable average bond strength density (Table 1). This may be an irreversible phenomenon where the rate of disulfide bond destruction exceeds the rate of formation of disulfide bonds leading to a progressively weak network (Wall, 1971). This transition influences the shape of the stress wave and results in progressively increasing distortions as the strain and the frequency both increase. We also observe that the transition strain becomes progressively larger as the dough undergoes mixing from Phase 1 to Phase 4.

The change in G′ and G″ values in the linear and non-linear region versus frequency are shown in Fig. 2. In the linear region, the difference between G′ and G″ values are higher compared to the difference in the non-linear region at all phases of mixing showing that dough is a highly elastic material when it is not overstretched as in the SAOS region but the G′ and G″ values progressively are closer in magnitude and at the larger strains as the gluten network softens and ultimately G′ overtakes G″ because the gluten network loses its integrity resulting in a progressively less elastic material. Faubion and Hoseney (1990) have referred to this as the transition from a “viscoelastic solid to a viscoelastic liquid”. The G′ and G″ values of the sample in the 1st phase of mixing showed slightly higher values compared to the one in the 2nd phase of mixing, especially at 1 rad/sec and 10 rad/sec frequency values. In the 1st phase of mixing, since the gluten network formation is not complete, the dough sample still does not have the desired viscoelasticity and might be more elastic compared to the 2nd phase of mixing. Gluten network formation was not completed in the 2nd phase of mixing and an increase was observed in the G′ and G″ values of the sample obtained both from the 3rd and the 4th phase of mixing, which indicates that the dough development continued after the 2nd phase of mixing.

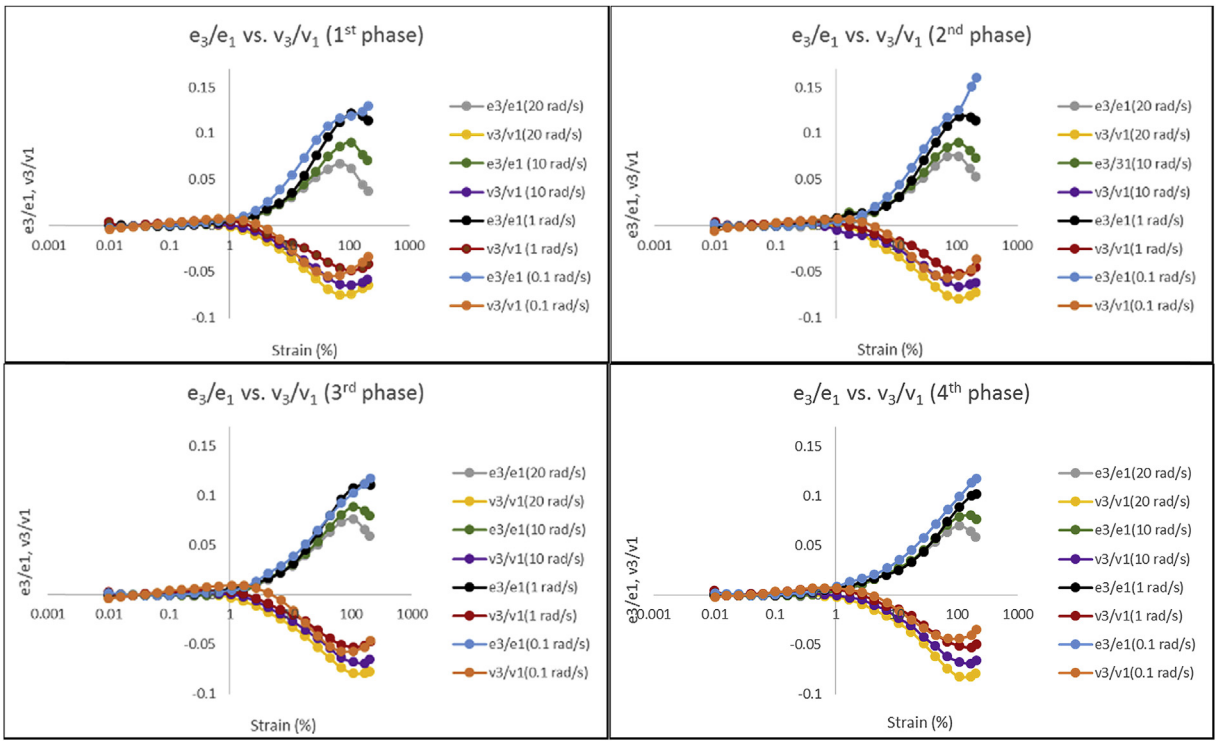

Fig. 6. The changes in e_3/e_1 and v_3/v_1 values of hard dough samples at different frequency values.

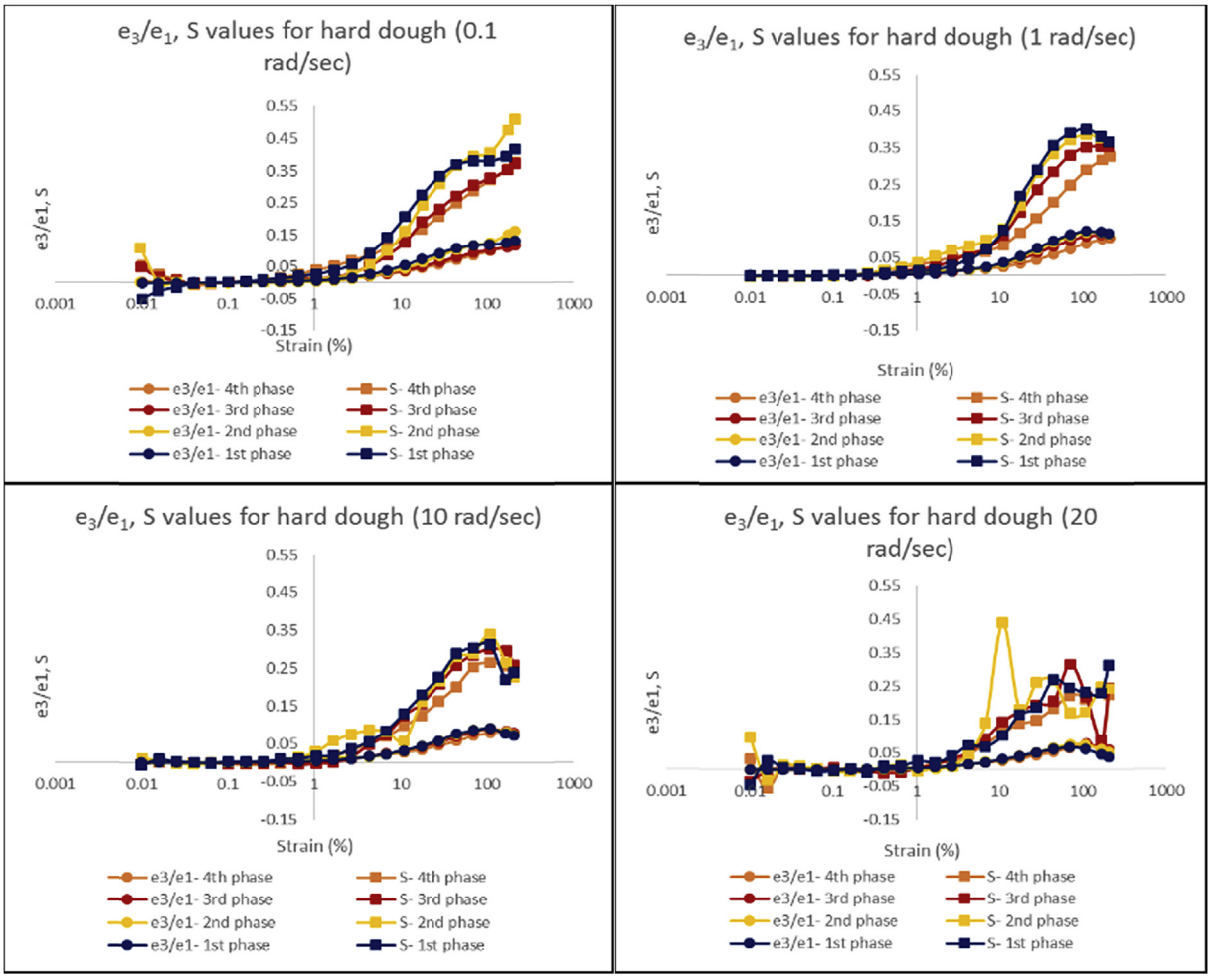

Fig. 7. e_3/e_1 and S Values of Hard Dough Samples.

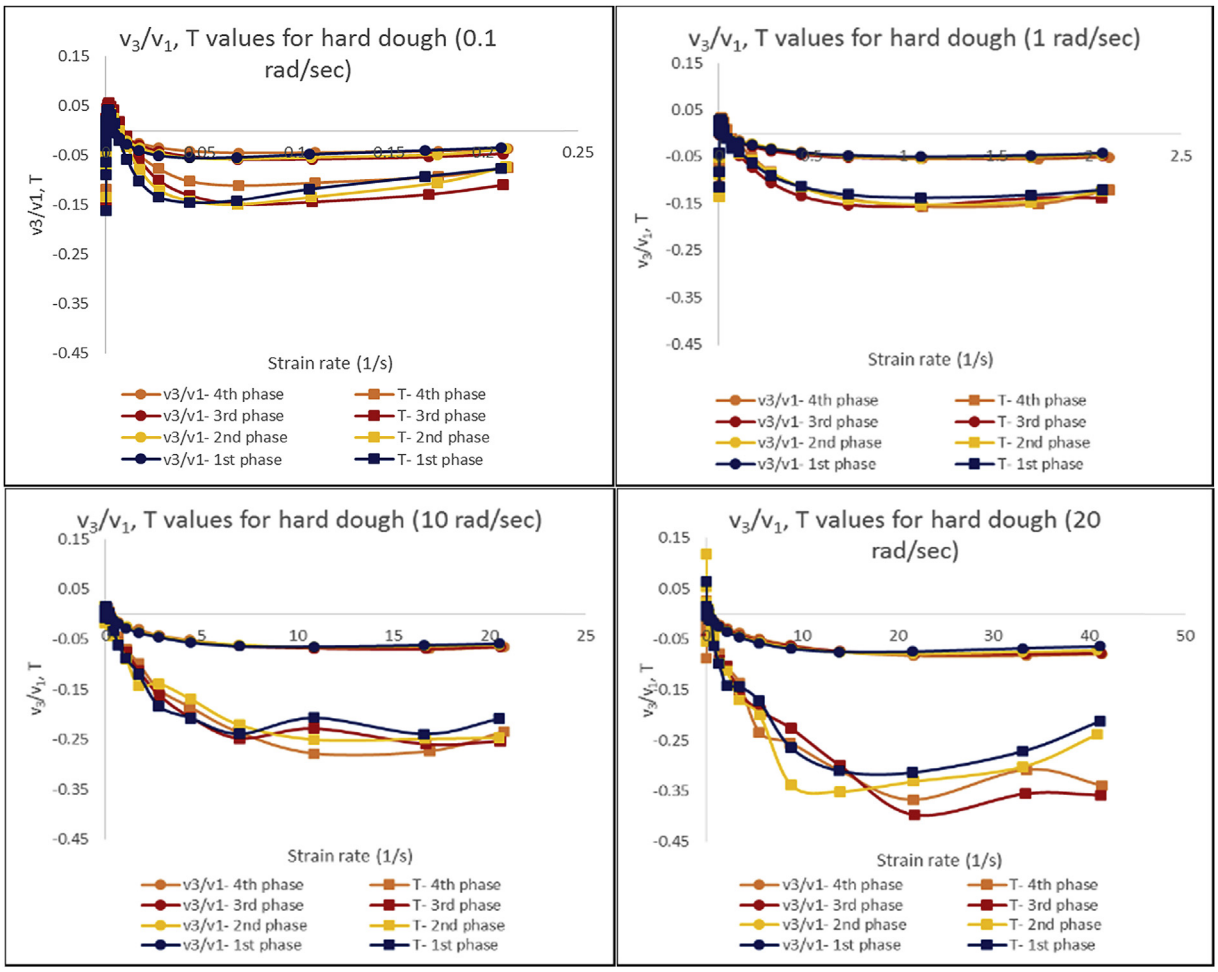

Fig. 8. v_3/v_1 and T values of Hard Dough Samples.

3.2. Analysis of the behavior of Lissajous curves

3.2.1. Analysis of the elastic component of stress

We deconvoluted the total stress oscillation into an elastic oscillation and a viscous oscillation by considering the in phase and out of phase component of stress (Lauger and Stettin, 2010; Hoyle et al., 2014, Stadler et al., 2008, Carmona et al., 2014; Ptaszek, 2015; Ewoldt and McKinley, 2010). The Lissajous-Bodwitch curves for the elastic component of stress are plotted in the form of normalized stress and normalized elastic stress vs. normalized strain for each frequency and for the four phases of dough mixing. This figure enables understanding of the intracycle rheological behavior of hard wheat flour dough as the amplitude of strain increases in different curves for all strains (0.01, 0.06, 1.6, 11, 28, 44, 70, 105, and 200%) where the data was obtained. We superimposed all the strain curves and we show the comparison just for the 1st and 4th phases of mixing to be able to carefully deconvolute the changes occurring during mixing (Fig. 3).

In the Lissajous curves a circular trajectory is observed for highly viscous relatively inelastic materials. The response of a highly elastic material appears either as a straight line or a narrow elliptical response. Elliptical trajectories indicate linear viscoelastic responses for solid-like materials (Ewoldt et al., 2007). In the linear region at small strains, the curves are perfect ellipses and show the complete reversible recovery of the structure during a cycle. As we approach the non-linear strains while the strain sweeps show the transition strain to be very low, the Lissajous curves display perfect ellipses up to significantly higher strains. This could be due to the reorientation of the starch structure without actually dismantling the protein network that maintains elasticity and intracycle linearity. As the strain increases, intracycle strain stiffening is being observed at all frequencies as a result of the stiffening in the gluten network. This phenomenon is very similar to what we observe in start-up of steady shear flow in many food materials (Dickie and Kokini, 1982, 1983; Kokini and Dickie, 1981). The loops started to get wider as the frequency decreased, which shows that dough behaves more like an elasto-viscous material at low frequencies. This is attributed to the inhomogeneity in the distribution of crosslinks enabling a significant part of the matrix to be loosely held together in contrast to observations at higher frequencies where the network is fully stretched and held tightly and elastically together. At the largest frequency, the intracycle strain stiffening occurred faster. Similarly, the Lissajous curves show narrower elliptical trajectories as the mixing proceeds as shown in Fig. 3a (1st phase) and Fig. 3b (4th phase). This is a reflection of the development of the viscoelastic network of gluten in dough up to the departure time where the onset of breakdown is known to occur.

3.2.2. Analysis of the viscous component of stress

In Fig. 4, we plot the out of phase component of the stress vs. the strain rate in order to obtain the viscous Lissajous curves. As strain and frequency increase the Lissajous curves become progressively

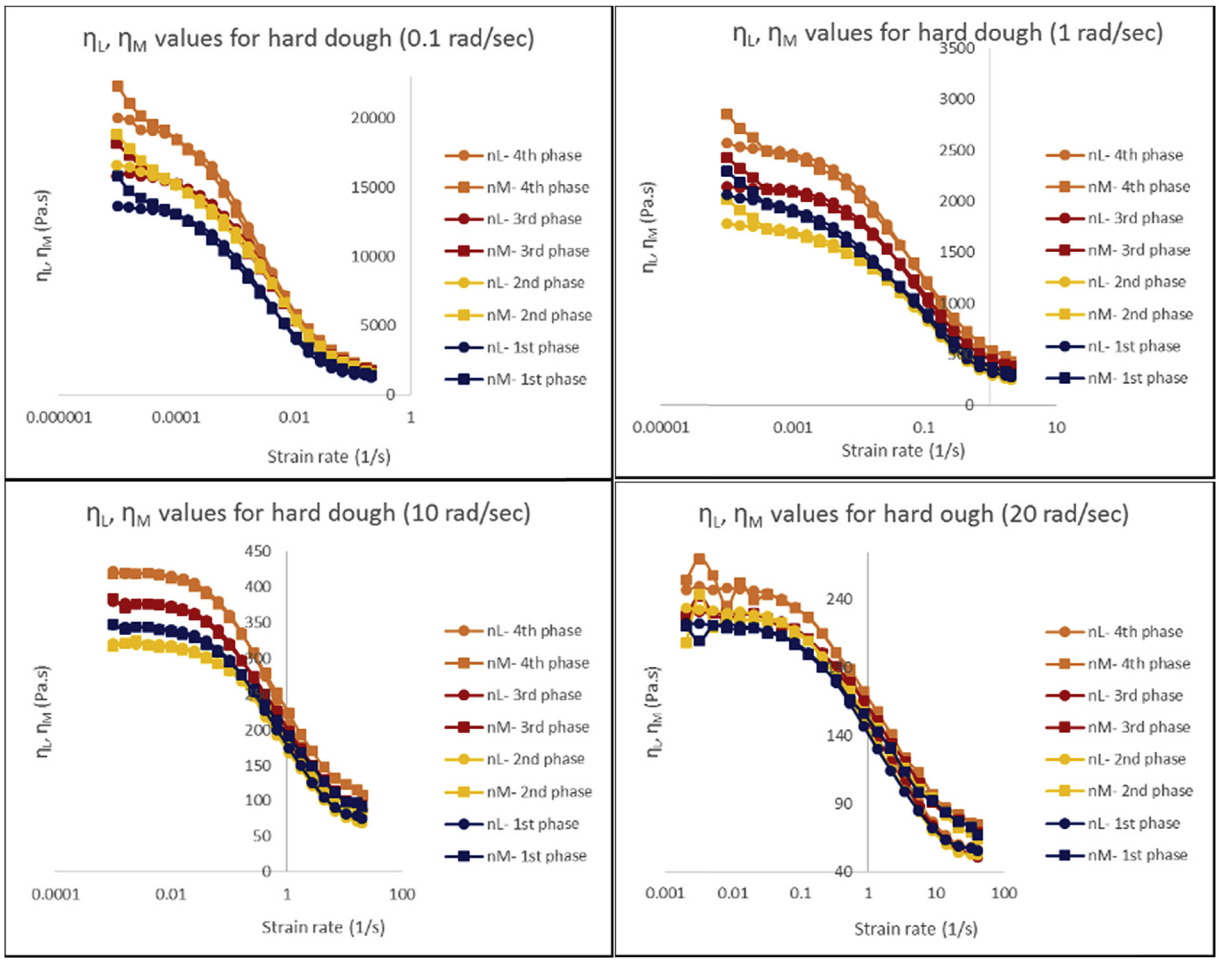

Fig. 9. Large (η_L) and Minimum Strain Rate Viscosity (η_M) Change vs. Strain Rate Values for Hard Dough Samples.

more elliptic. The figures clearly show that the larger contribution to the stress wave comes from the elastic component. Non-linearities are more obvious in the elastic component compared to the viscous component. Both elastic and viscous data support one another and offer deeper and more precise insights into the non-linear behavior of wheat flour dough.

3.3. *Non-linear rheological elastic properties of dough as a function of mixing phase*

Additional information is obtained by analyzing the large strain modulus G_L and the ratio e_3/e_1. The large strain modulus, G_L, increased with mixing after the 2nd phase (Fig. 5). Hard wheat flour particles are dense and water penetrates the particles slowly through diffusion. The mixing process facilitates diffusion because it reduces the mass transfer coefficient at the water particle interface (Hoseney, 1994). As more and more of the free water is used to hydrate the protein and starch, resistance of the system to applied extension is increased progressively. Thus, the height of the mixing curve gradually increases to a peak (Hoseney, 1994) and then slowly decreases with increasing hydration. SEM images in the study of Roman-Gutierrez et al. (2002) showed that hard wheat flour particles appear to swell with increasing mixing time. The study of Rao et al. (2000), consistent with our own observations showed that extra-strong wheat cultivars had greater elasticity and needed more mixing. They also show longer relaxation times than moderately strong wheat cultivars. All these studies explain why G_L values increase as the mixing proceeds at all frequency levels. The gluten matrix is able to hold the dough structure together and the large strain modulus seem to be close in magnitude because the matrix does not break as the both the strain and the frequency increase.

If the large strain modulus G_L is greater than the minimum strain modulus G_M, then the response is strain stiffening, because strain stiffening (S) is defined as; $S \equiv (G'_L - G'_M)/G'_L$ (Ewoldt et al., 2008). So, G_L and G_M values both determine the strain stiffening/softening behavior of the samples. G_L and G_M values decreased as the frequency decreased, however, they increased as the mixing proceeded from the 1st phase to the 4th phase at all strains. As the sample reached the non-linear region, G_L and G_M values decreased and S values increased, suggesting more strain stiffening behavior. As the mixing proceeds from the 1st to the 4th phase, the point, where the dough structure breaks down and turns to a decreasing level of strain stiffening behavior, retards. That can be observed in Fig. 6. On the other hand, G_L values decreased as the frequency decreased at all the stages of Farinograph mixing. Ewoldt et al. (2008) states that intracycle strain stiffening occurs if $S > 0$ and $S < 0$ corresponds to intracycle strain softening. This information shows that the hard dough samples showed strain stiffening behavior at all phases of mixing and at all applied frequency values, especially in the transition and non-linear regions.

e_3/e_1 values brought a deeper insight and showed that the hard dough samples obtained from different phases of Farinograph mixing showed strain stiffening up to a strain value of around 100% at

frequencies 20, 10, and 1 rad/sec. Gluten network in hard dough samples might be showing resistance to the applied strain up to a maximum point (Fig. 6), however since the frequency level is also high, the network might be undergoing bond ruptures as the strain keeps increasing. And as a result; the dough sample represents a high degree of strain stiffening at the beginning, followed by a decrease in the rate of strain stiffening after a certain strain value at all the frequency levels excluding the lowest frequency applied in our experiments (0.1 rad/sec). The intensity of the strain stiffening behavior increased as the frequency decreased. This is very new information that is not accessible quantitatively with any other method. Dough is known to partially recover after being stretched rapidly and the force is immediately released (Delcour and Hoseney, 2013). However, in the measurements we have carried out, the dough samples might not have the time to recover in the high frequencies due to the oscillatory deformation. As a result, they showed a maximum in the strain hardening behavior after a critical strain depending on the applied frequency and then a reduction was observed in the degree of strain stiffening. The magnitude of the v_3/v_1 ratio increases from 0 in the linear region to about 0.8 in the non-linear region where a maximum is observed. Beyond this maximum at higher strains the ratio begins to decrease. This is attributed to the softening in the gluten network and also the disruption in the starch network at large strains and frequencies. When we compare the v_3/v_1 and e_3/e_1 ratios as a function of strain it is clearly seen that the non-linearity is more pronounced in the elastic component compared to the viscous component.

3.4. Non-linear viscous properties of dough as a function of mixing phase

In contrast to e_3/e_1 values, v_3/v_1 values start to increase after a specific strain value around 100% suggesting shear thickening behavior after this strain value. All e_3/e_1 values are positive (+), while v_3/v_1 values are negative (−) in the non-linear region. Strain stiffening in the elastic response is indicated $e_3 > 0$ and shear thinning behavior is indicated by $v_3 < 0$ as the magnitude of strain increases. The magnitude of e_3/e_1, v_3/v_1 provide a quantitative measure of the degree of nonlinearity and give equivalent interpretation to e_3 and v_3, since e_1 and v_1 are always positive and correspond to the linear elastic and viscous responses in the curve (Ewoldt et al., 2007, 2008). Clearly, hard dough samples show strain stiffening ($e_3/e_1 > 0$) and shear thinning ($v_3/v_1 < 0$) behavior at all stages of Farinograph mixing. As the frequency decreased, these values both showed increase for all the hard dough samples obtained at different stages of Farinograph mixing.

Strain stiffening ratio (S) values of the hard dough samples at different stages of mixing showed a correlation with the e_3/e_1 values at all frequencies, while similar correlation was observed for shear thickening ratio (T) and v_3/v_1 values (Figs. 7 and 8). Negative T values were observed for all the dough samples at all frequency levels, which is an indication of intracycle shear thinning behavior (Fig. 8). Shear thinning behavior starts to increase as the frequency increases.

Large (η_L) and minimum strain rate (η_M) viscosity values were plotted in Fig. 9. η_L (at maximum stretch) and η_M (at the beginning of each oscillation cycle) values are very close to each other and decreases as the frequency increases. While the highest values for G_L were obtained at 20 rad/sec frequency level, the lowest values were obtained for η_L and η_M values at the same frequency. η_L and η_M values generally followed the same trend in all the stages of mixing at all applied frequencies and their magnitude in the 4th phase of Farinograph mixing were higher than of the ones at different stages of mixing at all frequency levels in the non-linear region, similar to G_L and G_M values. η_L values showed a progressive decrease at all frequency levels as the mixing proceeds until the 4th phase. η_L values increased as the frequency decreased from 20 rad/sec to 0.1 rad/sec gradually.

4. Conclusions

We have gained new insights into the non-linear rheological behavior of wheat flour doughs such as intracycle behavior of dough in both linear and non-linear region. The in phase and out of phase stress components evaluated through LAOS offer additional understanding and demonstrate that the in phase component of dough is affected much more significantly than the out phase component in the non-linear region upto 200% strain. Evaluating the Lissajous curves for the elastic and viscous components of hard wheat flour dough enabled us to understand that the elastic component started to behave more elastically dominated and the viscous component of dough behaved more viscous as mixing proceeded from the 1st to the 4th phase. For this reason, the dough sample gained a sticky character at the last phase of mixing which was reflected as wider Lissajous curves for the viscous component (starch phase). However, the development in the gluten network (elastic component) was still proceeding that results in narrower Lissajous curves at the 4th phase. LAOS parameters (e_3/e_1, v_3/v_1, G_L, G_M, η_L, η_M, S and T) showed that, the gluten network has time to stretch and reaches its limit in terms of its ability to elastically deform at the lower frequencies. These findings are consistent with Ng et al. (2011)'s findings on gluten gels. We then studied Lissajous curves and we saw the previously observed intracycle strain thickening to occur with dough as well at all phases of Farinograph mixing. The resulting LAOS parameters showed a strong strain dependence supporting the elastic Lissajous data and demonstrating the strain stiffening behavior and also consistent with the viscous Lissajous curves demonstrating the shear thinning behavior. Similarly, positive S values showed that the hard dough samples obtained at different phases of Farinograph mixing showed strain stiffening behavior at all applied frequencies in the non-linear region (0.01–200% strain range); while T values with negative results represented that the samples showed shear thinning behavior at the same time. G_L values also supported the data obtained with the Lissajous curves. Dough development was still continuous at the last phase of Farinograph mixing, since G_L values were higher at all applied frequencies for the hard dough sample obtained at the 4th phase of mixing compared to the samples obtained at the previous stages of mixing, These are completely new insights into dough rheology and have not been studied in the content of dough before.

LAOS data can also be useful in terms of adjusting formulations, process parameters i.e. time required for mixing or fermentation, temperature for bakery products. Because dough is exposed to a range of strain changing from 100% to 500,000% strain during processing (Menjivar, 1990) and LAOS tests applied on dough enable to determine the maximum strain levels that dough can handle. Therefore, adjusting the process parameters depending on the data obtained through LAOS tests result in producing bakery products with better quality.

Acknowledgements

This research was partly funded by USDA Hatch funds, the William R. Scholle Foundation, a Fellowship to Gamze Yazar from The Scientific and Technological Research Council of Turkey (TUBITAK). The authors gratefully acknowledge all of these funding sources which made this research possible.

References

AACC, 2000. Farinograph Method for Flour, AACC Method 54–21. Approved Methods of the AACC, Vol. II. American Association of Cereal Chemists Inc (USA).

Amemiya, J.I., Menjivar, J.A., 1992. Comparison of small and large deformation measurements to characterize the rheology of wheat flour doughs. J. Food Eng. 16, 91–108.

Carmona, J.A., Ramirez, P., Calero, N., Munoz, J., 2014. Large amplitude oscillatory shear of xanthan gum solutions. Effect of sodium chloride (NaCl) concentration. J. Food Eng. 126, 165–172.

Cho, K.S.K., Ahn, H., Lee, S.J., 2005. A geometrical interpretation of large amplitude oscillatory shear response. J. Rheol. 49, 747–758.

Connelly, R.K., Kokini, J.L., 2007. Examination of the mixing ability of single and twin screw mixers using 2D finite element method simulation with particle tracking. J. Food Eng. 79, 956–969.

Delcour, J.A., Hoseney, R.C., 2013. Principles of Cereal Science and Technology. AACC International Inc, St. Paul, MN.

Dickie, A.M., Kokini, J.L., 1982. Use of the Bird-Leider equation in food rheology. J. Food Process Eng. 5, 157–174.

Dickie, A.M., Kokini, J.L., 1983. An improved model for food thickness from non-Newtonian fluid mechanics in the mouth. J. Food Sci. 48, 57–61.

Duvarci, O.C., Yazar, G., Kokini, J., 2016. The comparison of LAOS behavior of structured food materials (suspensions, emulsions and elastic networks). Trends Food Sci. Technol. (accepted).

Ewoldt, R.H., Hosoi, A.E., McKinley, G.H., 2007. Rheological fingerprinting of complex fluids using large amplitude oscillatory shear (LAOS) flow. Annu. Trans. Nord. Rheol. Soc. 15, 3–8.

Ewoldt, R.H., Hosoi, A.E., McKinley, G.H., 2008. New measures for characterizing nonlinear viscoelasticity in large amplitude oscillatory shear. J. Rheol. 52 (6), 1427–1458.

Ewoldt, R., McKinley, G.H., 2010. On secondary loops in LAOS via self-intersection of Lissajous–Bowditch curves. Rheol. Acta 49, 213–219.

Ewoldt, R.H., 2013. Defining nonlinear rheological material functions for oscillatory shear. J. Rheol. 57 (1), 177–195.

Faubion, J.M., Hoseney, R.C., 1990. The viscoelastic properties of wheat flour doughs. In: Faridi, H., Faubion, J.M. (Eds.), Dough Rheology and Baked Product Texture. Van Nostrand Reinhold, New York, pp. 29–67.

Hoseney, R.C., 1994. Principles of Cereal Science and Technology. American Association of Cereal Chemists Inc, St Paul, MN.

Hoyle, D.M., Auhl, D., Harlen, O.G., Barroso, V.C., Wilhelm, M., McLeish, T.C.B., 2014. Large amplitude oscillatory shear and Fourier transform rheology analysis of branched polymer melts. J. Rheol. 58, 969–997.

Hyun, K., Wilhelm, M., Klein, C.O., Cho, K.S., Nam, J.G., Ahn, K.H., Lee, S.J., Ewoldt, R.H., McKinley, G.H., 2011. A review of nonlinear oscillatory shear tests: analysis and application of large amplitude oscillatory shear (LAOS). Prog. Polym. Sci. 36, 1697–1753.

Kim, Y.-R., Cornillon, P., Campanella, O.H., Stroshine, R.L., Lee, S., Shim, J.-Y., 2007. Small and large deformation rheology for hard wheat flour dough as influenced by mixing and resting. J. Food Sci. 73 (1), 1–8.

Klein, C., Venema, P., Sagis, L., van der Linden, E., 2008. Rheological discrimination and characterization of carrageenans and starches by fourier transform-rheology in the non-linear viscous regime. J. Newt. Fluids 151, 145–150.

Kokini, J.L., Dickie, A., 1981. An attempt to identify and model transient viscoelastic flow in foods. J. Texture Stud. 12, 539–557.

Lauger, J., Stettin, H., 2010. Differences between stress and strain control in the non-linear behavior of complex fluids. Rheol. Acta 49, 909–930.

Liu, Q., Bao, H., Xi, C., Miao, H., 2014. Rheological characterization of tuna myofibrillar protein in linear and nonlinear viscoelastic regions. J. Food Eng. 121, 58–63.

Melito, H.S., Daubert, C.R., Foegeding, E.A., 2013a. Relating large amplitude oscillatory shear and food behavior: correlation of nonlinear viscoelastic, rheological, sensory and oral processing behavior of whey protein isolate/_-carrageenan gels. J. Food Process Eng. 36, 521–534.

Melito, H.S., Daubert, C.R., Foegeding, E.A., 2013b. Relationships between nonlinear viscoelastic behavior and rheological, sensory and oral processing behavior of commercial cheese. J. Texture Stud. 44, 253–288.

Menjivar, J.A., 1990. Fundamental aspects of dough rheology. Chap. 1. In: Faridi, H., Faubion, J.M. (Eds.), Dough Rheology and Baked Product Texture. AVI Publishing, New York.

Nam, J.G., Ahn, K.H., Lee, S.J., Hyun, K., 2010. First normal stress difference of entangled polymer solutions in large amplitude oscillatory shear flow. J. Rheol. 54 (6), 1243–1266.

Ng, T.S.K., McKinley, G.H., Ewoldt, R.H., 2011. Large amplitude oscillatory shear flow of gluten dough: a model power-law gel. J. Rheol. 55 (3), 627–654.

Ptaszek, P., 2015. A geometrical interpretation of large amplitude oscillatory shear (LAOS) in application to fresh food foams. J. Food Eng. 146, 53–61.

Rao, V.K., Mulvaney, S.J., Dexter, J.E., 2000. Rheological characterization of long- and short- mixing flours based on stress-relaxation. J. Cereal Sci. 31, 159–171.

Roman-Gutierrez, A.D., Guilbert, S., Cuq, B., 2002. Description of microstructural changes in wheat flour and flour components during hydration by using environmental scanning electron microscopy. Lebensm. Wiss. Technol. 35, 730–740.

Schulentz, E.J., Steffe, J.F., Ng, P.K.W., 2000. Rheology and microstructure of wheat dough developed with controlled deformation. J. Texture Stud. 31, 41–54.

Stadler, F.J., Leygue, A., Burhin, H., Baily, C., 2008. The potential of large amplitude oscillatory shear to gain an insight into the long-chain branching structure of polymers. Polym. Prepr. 49, 121–122.

Wall, J.S., 1971. Disulfide bonds: determination, location, and influence on molecular properties of proteins. J. Agric. Food Chem. 19 (4), 619–625.

Wilhelm, M., 2002. Fourier-Transform rheology. Macromol. Mater. Eng. 287, 83–105.

Wilhelm, M., 2011. New methods for the rheological characterization of materials. Chem. Eng. Process. 50, 486–488.